ESKİŞEHİR TEKNİK ÜNİVERSİTESİ BİLİM VE TEKNOLOJİ DERGİSİ
B- TEORİK BİLİMLER

Eskişehir Technical University Journal of Science and Technology B- Theoretical Sciences

Estuscience – Theory, 2025, 13 [1] pp. 7-23 , DOI:10.20290/estubtdb.1501639

RESEARCH ARTICLE

ANALYSIS BY DFT, ADME AND DOCKING STUDIES OF N'-(4-HYDROXY-3-METHOXYBENZYLIDENE)NAPHTHO[2,3-B]FURAN-2-CARBOHYDRAZIDE

Kenan GÖREN [1, *], Mehmet BAĞLAN [2], Ümit YILDIKO [3]

[1] Department of Chemistry, Kafkas University, Kars 36100, Turkey
kenangoren49@gmail.com - *0000-0001-5068-1762*

[2] Department of Chemistry, Kafkas University, Kars 36100, Turkey
mehmetbaglan36@gmail.com - *0000-0002-7089-7111*

[3] Department of Bioengineering, Kafkas University, Kars 36100, Turkey
yildiko1@gmail.com - *0000-0001-8627-9038*

Abstract

In this study, N'-(4-hydroxy-3-methoxybenzylidene)naphtho[2,3-b]furan-2-carbohydrazide (HMFC) compound containing Schiff base was theoretically examined. The HMFC molecule was calculated theoretically using the 6-311G(d,p), B3LYP/B3PW91 basis sets and methods. The energy gap of the molecule, the lowest unoccupied molecular orbital (LUMO), and the highest occupied molecular orbital (HOMO) values were calculated using the identical set and two distinct methods. The HMFC compound's molecular stability was examined by applying the natural bond orbital (NBO) study. The Nonlinear optical Properties (NLO) of HMFC molecule, thermodynamic parameters, and Molecular Electrostatic Potential Maps (MEP) were calculated. Molecular docking study of the HMFC compound was performed by downloading two different enzyme codes (PDB ID: 1T46 and PDB ID: 3SXR) from PDB (Protein Data Bank) and examining in silico the cancer-associated proteins to analyze the potential anticancer activity. In the docking analysis, it showed a score of -7.356 kcal/mol for the 1T46 enzyme code in the compound, while it showed a score of -6.866 kcal/mol for the 3SXR enzyme code. Whether the HMFC molecule has drug properties was analyzed using the absorption, distribution, metabolism, and excretion (ADME) approach.

Keywords

Molecular Docking Analyses,
Natural Bond Orbital Analyses,
Molecular Electrostatic Potential Maps,
Nonlinear Optical Properties

Time Scale of Article

Received :15 June 2024
Accepted : 25 November 2024
Online date : 28 February 2025

1. INTRODUCTION

In 1864, Hugo Schiff described the condensation of an amine with an aldehyde to produce a Schiff base. Schiff bases, having the existence of the imine group, are used to clarify the transformation process of the racemization reaction in biological systems [1]. Its azomethine linkage (>C=N-) gives it anticancer, antibacterial, antifungal, and herbicidal activities, among other effects, in biological systems. because of their potent antiviral, antifungal, and antibacterial qualities, several Schiff derivatives are useful therapeutic medications [2]. The structure-activity link between biomolecules and pharmacological molecules is also often understood using Schiff bases and their analogs as model compounds. Schiff bases are considered interesting medicinal compounds for the creation of novel drugs because of their many biological uses, particularly in the case of hydrazone derivatives [3-5]. Schiff bases have been extensively studied by many researchers due to their antibacterial, antiviral, antimalarial, anti-inflammatory, and antioxidant properties. Moreover, it has been documented that Schiff bases coupled

*Corresponding Author: kenangoren49@gmail.comx

with benzothiazole provide unique physiologically active molecular hybrids with noteworthy chemotherapeutic effects [6]. For instance, Schiff bases are essential to the advancement of coordination science since they readily create stable structures with the majority of metals and anticancer medications. Schiff-based chemicals tend to become more anti-cancer when they form complexes with metal ions [7].

The popularity of DFT-based methods is due to their wider range of applications and significantly cheaper computational cost compared to more accurate wave function-based methods [8]. These methods can yield findings that are sufficiently precise for a wide range of chemical systems (both in regard to size and complexity). Particularly in this regard, LR-TD-DFT20 has been shown to be a potent and adaptable method for treating aroused states [9].

Computer-aided quantum chemical calculations are performed using molecular modeling programs to help experimental research or to forecast the outcomes to be attained without completing experimental experiments [10]. The creation of effective programs that can compute molecular parameters including dipole moment, total energy, optimal shape, and vibration wave numbers is the main goal of these programs. These computations are based on quantum mechanics [11]. Atoms and molecules were subjected to the principles of quantum mechanics as soon as quantum theory was developed. In theory, quantum theory allows one to compute any molecule's chemical property. While there are numerous applications for prediction through computation, experimental approaches are still a valuable means of determining a compound's structure and chemistry [12].

The main purpose of this study, the Schiff base derivative N'-(4-hydroxy-3-methoxybenzylidene)naphtho[2,3-b]furan-2-carbohydrazide (HMFC) molecule was theoretically investigated using the 6-311G(d,p), B3LYP/B3PW91 basis sets and methods. The DFT method was used to calculate the chemical descriptors HOMO-LUMO gap, and HOMO-LUMO, which are regarded as markers of the examined compounds' chemical reactivity. A study on molecular docking has been carried out against the molecule to shed more light on its biological application; The study reports on their binding affinity to the pathogen's protein and shows their capacity to bind with the protein through a comparative docking score. Finally, ADME analysis was performed in the study. ADME analysis findings suggest that these compounds may possess intriguing features for use in pharmaceuticals, which might make them useful as active components in novel pharmaceuticals. According to the ADME research, it has an excellent absorption profile of 79.99%, and the field that produces safe and effective medications may find use for the literature study's findings.

2. MATERIALS AND METHODS

The 6-311G(d,p), B3LYP/B3PW91 basis sets and methods were the basis sets and methods used in study for all DFT calculations performed in Gaussian 09 software. We used a semi-empirical conformational analysis method. The initial step of computer analysis was to optimize the final molecule's form. It specifically calls for low energy sensitivity to modifications in molecules caused due to the nuclear location shifting of the molecule. The best molecular structure geometries, vibration frequencies, and energies of HMFC chemical were determined using the DFT method in Gaussian 09 software. The DFT method has been used to generate the Lee's-Yang-Parr correlation function using the 6-311G(d,p) basis set-based computer package [13]. The visualization and input files have been prepared and imported using GaussView 6.0.16 and ChemBio Ultra Drive 3D. To identify the specific binding location and mechanism of the ligand on the protein, molecular docking research was conducted using the Maestro Molecular Modeling platform (version 11.8) [14] of the Schrödinger, LLC model and waited for the wizard module to get data on protein preparation. In the meantime, a crystal structure formed from the separation of all water molecules. The protein ion balance was restored by returning to this module and selecting the flexible protein-binding active site. Designed to serve as the foundation of the receptor network module, network boxes enable adaptable docking by creating networks at the

locations where proteins bind. Receptor connection modules are built on network boxes, which enable flexible docking through the formation of networks at protein binding sites. The lowest energy arrangement represents the strongest affinity for binding. Ultimately, the ADME analysis of HMFC molecule in this work was conducted using the online database SwissADME (http://www.swissadme.ch).

3. RESULTS AND DISCUSSION

3.1. Structure Details and Analysis

Using the Density Function Theory (DFT) method and polarizing functions added to eliminate the polarization effect, the approximate geometry of this molecule in gas phase was drawn using the GaussView 6.0.16 molecular imaging program. The electron density in excited ionic molecules is higher than that of the ground-state molecule. Geometry optimization with restricted closed shell calculations, in which each electron pair is forced to occur in a single orbit, was used to determine the space settlements and space structure of the atoms in the compound using the 6-311G(d,p) basis set, which includes diffuse functions added to model the dispersed state [15, 16]. As a result, theoretical calculations were made for bond lengths (Å), bond angles (°), and dihedral angles (°). Table 1 presents the structure's bond length and bond angles as determined using the 6-311G(d,p), B3LYP/B3PW91 basis sets and methods. With values of 1.37 and 1.41 Å to C-O, the C-C bond lengths for B3PW91 and B3LYP are 1.36-1.53 Å and 1.37-1.54 Å, respectively. The aromatic ring's C-H lengths are around 1.08 Å in value. The range of all C-C-C angles is 101° to 122°. We noticed that some dihedral angles produced negative angle-degree outcomes when atoms were used as dihedral bonds in the Gaussian 09 software. These calculated values were assigned values based on where the atoms were located inside the bonds. We saw very slight variations in the dihedral bond values between the two methods. When we compared the theoretical results obtained with two different methods, we observed that they were close to each other and compatible.

Table 1. Theoretically optimized geometric parameters of the molecule HMFC

Bond Lengths	**B3PW91/ 6-311G(d,p)**	**B3LYP/ 6-311G(d,p)**	**Bond Lengths**	**B3PW91/ 6-311G(d,p)**	**B3LYP/ 6-311G(d,p)**
C4-C5	1.43121	1.43462	**N17-C18**	1.28282	1.28450
C4-C7	1.41993	1.42297	**C18-C19**	1.47151	1.47486
C7-C8	1.43121	1.36663	**C21-C22**	1.38644	1.38833
C8-C9	1.36533	1.41309	**C22-O25**	1.34960	1.35526
C8-O11	1.37052	1.37659	**C23-O26**	1.36379	1.36976
C9-C13	1.50489	1.50849	**O26-C27**	1.41803	1.42564
C12-C13	1.53899	1.54601	**O25-H42**	0.96607	0.96718
C12-C14	1.53700	1.54201	**N16-H37**	1.01553	1.01460
C14-N16	1.36833	1.37178	**C18-H38**	1.08899	1.08826
N16-N17	1.35853	1.36760	**C24-H41**	1.08227	1.08032
Bond Angles	**B3PW91/ 6-311G(d,p)**	**B3LYP/ 6-311G(d,p)**	**Bond Angles**	**B3PW91/ 6-311G(d,p)**	**B3LYP/ 6-311G(d,p)**
C6-C5-C10	122.66744	122.76053	**N16-N17-C18**	118.45382	118.55801
C7-C8-O11	124.77683	124.73284	**N17-C18-C19**	131.07090	131.58017
C9-C8-O11	112.17530	112.19842	**C21-C22-O25**	120.58918	120.44303
C9-C12-C13	101.77366	102.01231	**C23-C22-O25**	120.05667	113.64148
C12-C14-N16	113.39116	113.39530	**C23-O26-C27**	118.28394	118.55989
Planar Bond Angles	**B3PW91/ 6-311G(d,p)**	**B3LYP/ 6-311G(d,p)**	**Planar Bond Angles**	**B3PW91/ 6-311G(d,p)**	**B3LYP/ 6-311G(d,p)**
C1-C6-C5-C10	-179.94428	-179.95212	**C12-C14-N16-N17**	177.78572	177.90167
C5-C10-C9-C13	-177.84628	-178.05155	**C14-N16-N17-C18**	178.90535	178.52697
C4-C7-C8-O11	179.54733	179.61311	**C21-C22-C23-O26**	-179.99596	-178.95493
C8-O11-C12-C14	-105.99149	-108.06229	**C22-C23-O26-C27**	-178.22383	-178.05634

3.2. Mulliken Atomic Charges

The most popular and traditional technique for load analysis is the Mulliken load distribution. Numerous applications contribute to its extensive use [17]. The idea behind this method, which derives from the linear integration of orbitals in atoms, is to distribute the wave functions to the atoms in the same proportion as the locations where two orbitals meet. This distribution, however, does not accurately depict each element's electronegativity [18, 19]. Because it offers a wealth of information about a molecule's polarity, electronic structure, dipole moment of atomic molecules, charge distribution on atoms, acceptor pairs and donors that facilitate charge transfer in the structure, and different chemical structure properties, the Mulliken charge distribution method is a commonly used method [20]. Because the nearby element O15 possesses a notably electronegative property, the C14 carbon atom's mulliken atomic charge value was determined to be larger than that of different chemical structures. Table 2 displays further calculated Mulliken atomic charge measurements for the compound using the 6-311G(d,p), B3LYP/B3PW91 basis sets and methods. Some C atoms were found to be negatively charged, whereas other C atoms were found to be positively charged. Figure 1 compares some C atom values using the different methods. In the Figure 2 has been given the optimized geometry of the molecule HMFC using the B3PW91/6-311G(d,p) method and basis set. Because the nearby element O15 possesses a notably electronegative property, the C14 carbon atom's mulliken atomic charge value was determined to be larger than that of different chemical structures. Table 2 displays further calculated Mulliken atomic charge measurements for the compound using the 6-311G(d,p), B3LYP/B3PW91 basis sets and methods. Some C atoms were found to be negatively charged, whereas other C atoms were found to be positively charged. Figure 1 compares some C atom values using the different methods. Figure 2 has been given the optimized geometry of the molecule HMFC using the B3PW91/6-311G(d,p) method and basis set. When we compared the theoretical results obtained with two different methods, we observed that they took values far from each other and were not compatible.

Table 2. Mulliken atomic charges of the molecule HMFC

ATOMS	B3PW91/ 6-311G(d,p)	B3LYP/ 6-311G(d,p)	ATOMS	B3PW91/ 6-311G(d,p)	B3LYP/ 6-311G(d,p)
C5	-0.070	-0.059	**N16**	-0.298	-0.275
C6	-0.073	-0.065	**N17**	-0.200	-0.188
C7	-0.052	-0.043	**O25**	-0.405	-0.394
C8	0.205	0.205	**O26**	-0.386	-0.378
C9	-0.179	-0.162	**H28**	0.113	0.102
C10	-0.014	-0.014	**H29**	0.113	0.102
C12	-0.129	-0.086	**H30**	0.100	0.090
C13	-0.104	-0.081	**H31**	0.103	0.093
C14	0.379	0.350	**H32**	0.115	0.101
C18	0.106	0.092	**H33**	0.101	0.093
C19	-0.204	-0.175	**H34**	0.161	0.148
C21	-0.104	-0.091	**H35**	0.161	0.146
C22	0.180	0.173	**H36**	0.162	0.142
C23	0.148	0.143	**H37**	0.232	0.217
C24	-0.122	-0.108	**H38**	0.132	0.119

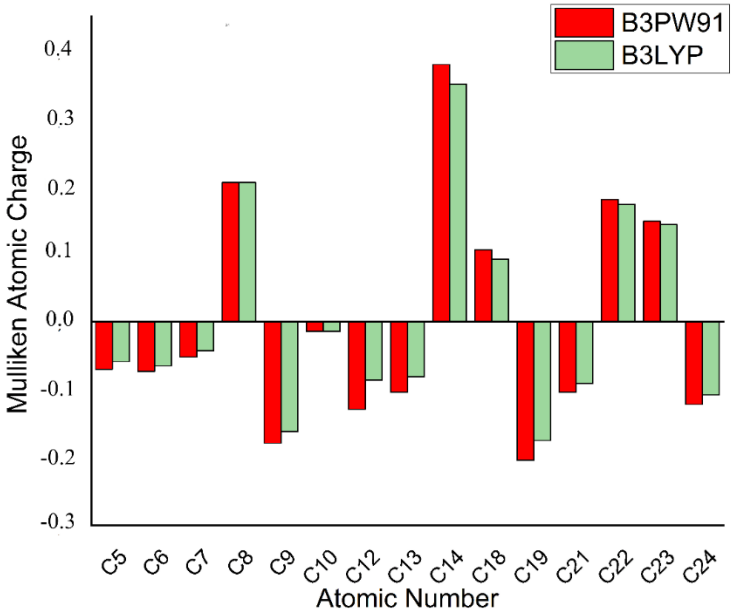

Figure 1. Mulliken atomic charge comparison for molecule HMFC

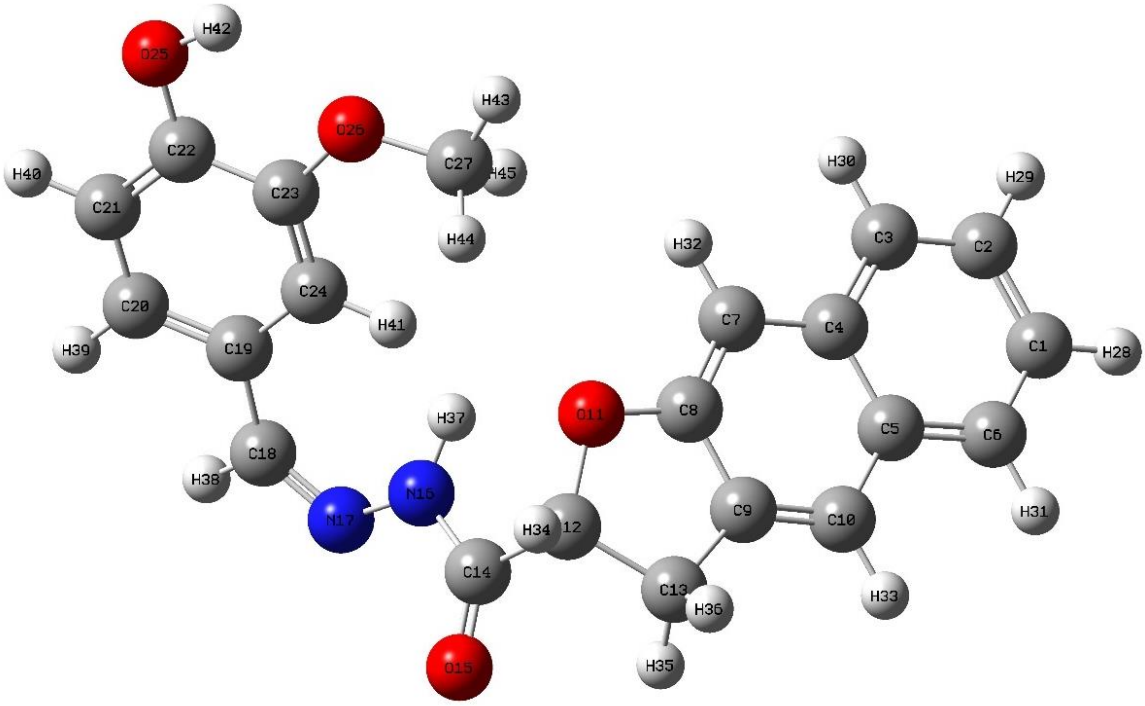

Figure 2. Optimized geometry display using the B3PW91/6-311G(d,p) method and basis set of molecule HMFC

3.3. HOMO and LUMO Analysis

Every molecule has two orbitals: LUMO and HOMO, according to molecular orbital theory. HOMO and LUMO orbitals are also known as leading orbitals because of their significance in chemical reactions [21]. The molecule's HOMO and LUMO energy levels differ from one another, signifying its chemical stability. The easier the reactant-reactant contact and reaction, the lower the ΔE energy difference, that is, the closer the energy levels of the interacting molecular orbitals are [22, 23]. It has been shown that

the energy values of molecules differ based on their hardness or softness, with soft molecules often having lower energy values than hard ones. The formulas for ionization energy, $I=-E_{HOMO}$, and electron affinity, $A=-E_{LUMO}$, represent the least amount of energy required to take one electron out of a molecule and the total energy that rises when an electron is added to the molecule in the gas phase, respectively [24]. $\eta=(I-A)/2$ gives the hardness value, which is a measurement of the blockage of charge transfer inside the molecule. The hardness of the HMFC molecule was calculated as 2.2754 with the B3PW91 method and 2.3249 with the B3LYP method. $S=1/2\eta$ represents the softness parameter, which is the opposite of hardness. The softness of the HMFC molecule was calculated as 1.1377 with the B3PW91 method and 1.1624 with the B3LYP method. When we examined the molecular hardness and softness values of the HMFC molecule calculated with two different methods, we observed that they were very close to each other and compatible. High-chemical-hardness molecules have little to no intramolecular charge transfer. The Mulliken electronegativity parameter, $\chi=(I+A)/2$, denotes a molecule's atom's capacity to draw electrons, except for the hardness and suppleness characteristics. Furthermore, he calculated the chemical capacity using $\mu=-(I+A)/2$ and the electrophilic index using $w=\mu 2/2\eta$ [25]. The densities of the HOMO and LUMO orbital representations for Molecule HMFC have been displayed in Figures 3 and 4. Table 3 shows that the B3PW91 method yielded HOMO-6.0340 eV/LUMO-1.4832 eV, while the B3LYP method yielded HOMO-5.9793 eV/LUMO -1.3295 eV.

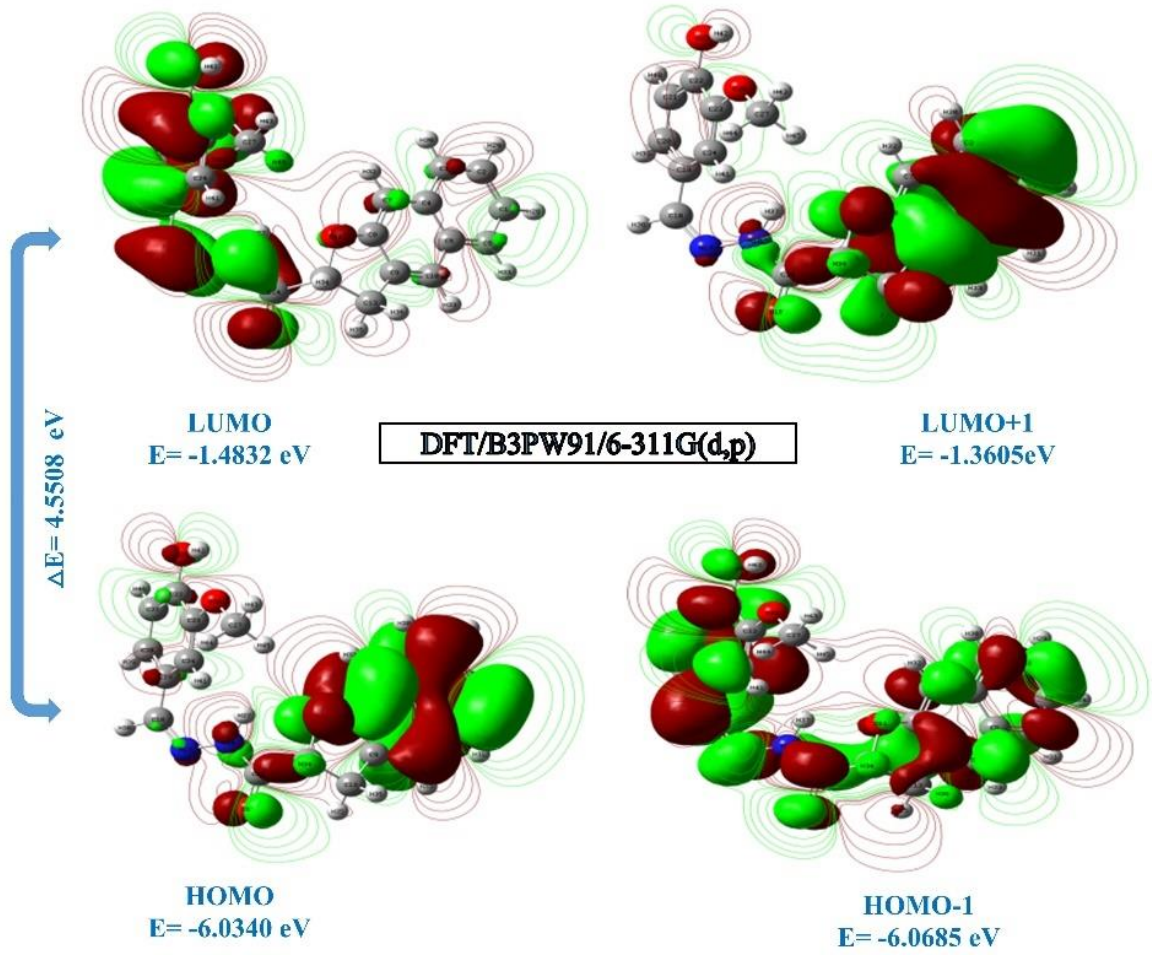

Figure 3. Pictures of frontier molecular orbitals using the B3PW91/6-311G(d,p) method and basis set

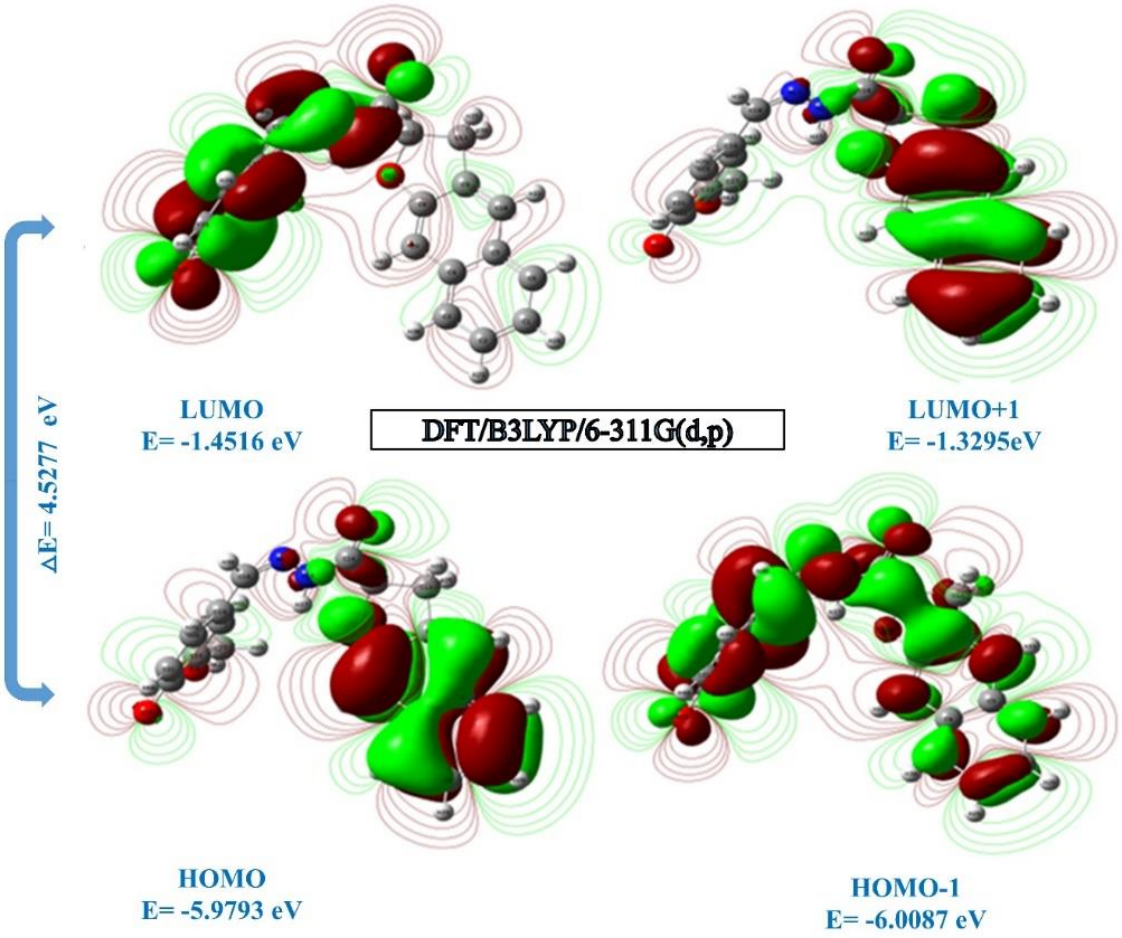

Figure 4. Pictures of frontier molecular orbitals using the B3LYP/6-311G(d,p) method and basis set

Table 3. Calculated quantum chemical parameters*(in eV) for low energy compatibilities by the 6-311G(d,p), B3LYP/B3PW91 basis set and methods of the HMFC molecule

Molecules Energy		**B3PW91/ 6-311G(d,p)**	**B3LYP/ 6-311G(d,p)**
E_{LUMO}		-1.4832	-1.4516
E_{HOMO}		-6.0340	-5.9793
E_{LUMO+1}		-1.3605	-1.3295
E_{HOMO-1}		-6.0685	-6.0087
Energy Gap	$(\Delta E)\lvert E_{HOMO}-E_{LUMO}\rvert$	4.5508	4.5277
Ionization Potential	$(I=-E_{HOMO})$	6.0340	5.9793
Electron Affinity	$(A=-E_{LUMO})$	1.4832	1.3295
Chemical hardness	$(\eta=(I-A)/2)$	2.2754	2.3249
Chemical softness	$(s=1/2\eta)$	1.1377	1.1624
Chemical Potential	$(\mu=-(I+A)/2)$	-3.7586	-3.6544
Electronegativity	$(\chi=(1+A)/2)$	1. 2416	1.16475
Electrophilicity index	$(\omega=\mu^2/2\eta)$	3.1043	2.8720

3.4. Molecular Electrostatic Potential (MEP)

Partial charges, electronegativity, and dipole moment are all connected to the molecular electrostatic potential surface. It is also favored for delineating hydrogen bond interactions and identifying nucleophilic and electrophilic reaction sites [26, 27]. In regions with low electron density, the proton is repelled by positive electrostatic potential, whereas The proton's attraction to the electron density is described by the negative electrostatic potential. The highest electrostatic potential, or nucleophilicity, is represented by the blue zone, while the smallest electrostatic potential, or electrophilicity, is represented by the red region [28]. The polarity of the molecule is connected to the wide gap in the molecular electrostatic potential scale. A molecule is said to be more polar if there are significant variations on the scale from red to blue. Figure 5 demonstrates that whereas oxygen and nitrogen atoms have negative potential zones that might be used for electrophilic assault, hydrogen atoms are more likely to have positive potential zones that could be used for nucleophilic attack.

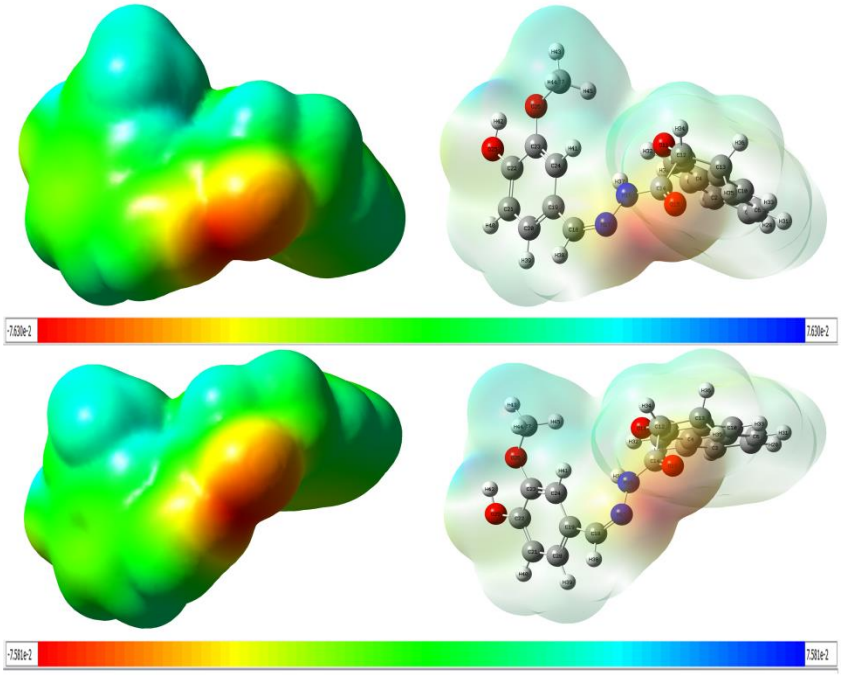

Figure 5. Molecular electrostatic potential surface of the molecule HMFC using the the 6-311G(d,p), B3LYP/B3PW91 basis sets and methods

3.5. Non-Linear Optical Properties (NLO)

NLO materials are widely used in many scientific fields, which has led to their increased attention in recent years. Good NLO qualities may be found in numerous photonic applications, including digital communications, signal processing, optical computing, sensors, and the creation of optical junction materials [29]. A molecule that is isolated has a dipole moment change when an external electrical field is present. In the equation of the total dipole moment, thus, aside from the permanent dipole moment, first- and second-order contributions appear [30]. First-order hyperpolarizability (β), which represents non-linear optical qualities, becomes significant if a stronger electric field is applied, whereas molecule polarizability (α), which represents linear optical properties, is considered if the applied electric field is weak [31]. Using the Gaussian 09 package software, one may determine a molecule's nonlinear optical characteristics by first calculating the energy of the optimized molecule and entering Polar=Enonly in the keyword area. Equations (1-3) are then used to compute the average molecule polarizability value from the output file in cartesian coordinates [32]. The polarization rises due to the simple alteration of

the electron distribution, which raises the β value. Furthermore, the attachment of acceptor-donor groups to the ends of the molecule influences the rise in the β value and the charge asymmetry. In addition to this, when the molecule is extended by adding more conjugated bonds, the β value which is dependent on the polarizability of the electrons in the π bond will also rise [33]. NLO analysis values have been given in Table 4. HMFC compound's first-order hyperpolarization values and molecular polarizability were determined in the 6-311G(d,p), B3LYP/B3PW91 basis sets and methods. After being translated from atomic unit (a.u.) to electrostatic unit (e.s.u.), the predicted molecular polarizability (α) and first-order hyperpolarizability (β) values were found to be $2.50\text{x}10^{-30}$ and $2.52\text{x}10^{-30}$ esu, respectively. When we compared the theoretical results obtained with two different methods, we observed that they were close to each other and compatible. The urea molecule is one of the model molecules used in studies on systems exhibiting NLO properties. The calculated μ and β values for both methods are approximately HMFC and seven times larger, respectively, than those of the typical NLO material "urea." The relatively large dipole moment and hyperpolarizability of HMFC compound may indicate that the substance can serve as a basic element for NLO materials.

$$\mu = \left(\mu_x^2 + \mu_y^2 + \mu_z^2\right)^{\frac{1}{2}} \quad (1)$$

$$\beta_{Total} = (\beta^2 x + \beta^2 y + \beta^2 z)^{1/2} \quad (2)$$

$$= [(\beta xxx + \beta xyy + \beta xzz)^2 + (\beta yyy + \beta yxx + yzz)^2 + (\beta zzz + \beta zxx + \beta zyy)^2]^{\frac{1}{2}} \quad (3)$$

Table 4. The dipole moments (Debye), polarizability (au), components, and total value of molecule HMFC are calculated using the 6-311G(d,p), B3LYP/B3PW91 basis sets and methods

Parameters	B3PW91/ 6-311G(d,p)	B3LYP/ 6-311G(d,p)	Parameters	B3PW91/ 6-311G(d,p)	B3LYP/ 6-311G(d,p)
μ_x	-0.5857	-0.5770	β_{XXX}	14.6593	12.8342
μ_y	0.7810	0.7399	β_{YYY}	4.8202	5.7078
μ_z	-2.1691	-2.1428	β_{ZZZ}	-11.0735	-10.7324
$\mu_{(D)}$	2.3786	2.3392	β_{XYY}	-6.8838	-8.2537
α_{XX}	-144.4681	-146.4085	β_{XXY}	52.8463	53.0179
α_{YY}	-133.8131	-136.1076	β_{XXZ}	50.0598	49.0202
α_{ZZ}	-171.5781	-172.2085	β_{XZZ}	-23.1842	-23.2474
α_{XY}	-7.9039	-7.8356	β_{YZZ}	2.3260	1.6622
α_{XZ}	-0.1837	-0.6591	β_{YYZ}	-26.3724	-25.7985
α_{YZ}	-8.8702	-8.8884	β_{XYZ}	3.3769	3.6133
α(au)	-169.172	-164.8441	**β(esu)**	$2.50\text{x}10^{-30}$	$2.52\text{x}10^{-30}$

3.6. NBO Analysis

The Gaussian 09 software contains a program that may be used to calculate NBO analysis, a commonly used method to look at how molecules interact with one another. This study yields the percentages of electrons present in various bonds for σ and π bonds as well as variations in the proportions of electrons on each atom in the s, p, and d orbitals [34]. Hybridizations that result in bond formation on atoms can also be achieved with this method. Furthermore, the NBO analysis looks at the orbitals' E(2) stabilization energies in addition to the interaction energies between orbitals and transition states. As is well known, π bonds are required to have p atomic orbitals of N, O, and C atoms by definition. It has been noted that the s orbital in the σ bond contributes less to the hybridization at the C atom than the other orbitals together [35]. O atoms saw far less of this alteration than C atoms did. As predicted, these modifications are almost nonexistent for π bonds. Table 5 presents the analytical findings for this data. By overlapping orbitals between bonding and antibonding orbitals, intramolecular hyperconjugative interactions facilitate intermolecular charge transfer, which leads to the molecular system's stability. The electron density in the antibonding orbitals increases as a result of these interactions, weakening the bond character. In the molecule under investigation, these bonds, together with their transition states and energy values, are as follows: π(C1-C2)→π*(C5-C6) 10.44 kcal/mol, π(C3-C4)→π*(C7-C8) 11.78

kcal/mol, π(C5-C6)→π*(C9-C10) 11.33 kcal/mol, and π(C9-C10)→π*(C7-C8) 11.24 kcal/mol. With stability energy data of 8.07, 13.92, 11.88, and 11.29 kcal/mol, respectively, the strongest interactions were found to be π(N17-C18)→ π*(C9), π(C19-C20)→ π*(N17), π (C22)→π*(C23-C24), and π*(23)→π* (C19-C20).

Table 5. Selected NBO results of molecule HMFC calculated using B3PW91/6-311G(d,p) method and basis set

NBO(i)	Type	Occupancies	NBO(j)	Type	Occupancies	E(2)[a] (Kcal/mol)	E (j)-E(i)[b] (a.u.)	F (i, j)[c] (a.u)
C1-C2	π	1.79417	**C5-C6**	π*	1.75478	10.44	0.31	0.051
C1-C6	σ	1.97579	**C5-C10**	σ*	1.96779	5.14	1.01	0.064
C2-C3	σ	1.97515	**C5-C6**	σ*	1.75478	5.22	1.00	0.065
C3-C4	π	1.75770	**C7-C8**	π*	1.84120	11.78	0.30	0.054
C4-C5	σ	1.96826	**C3-C4**	σ*	1.75770	3.16	1.25	0.056
C4-C7	σ	1.96127	**C8-O11**	σ*	1.98575	8.53	0.85	0.076
C5-C6	π	1.75478	**C9-C10**	π*	1.84522	11.33	0.31	0.054
C5-C10	σ	1.96779	**C1-C6**	σ*	1.97579	6.66	1.01	0.073
C7-C8	π	1.84120	**C9-C10**	π*	1.96741	12.04	0.33	0.056
C8-C9	σ	1.96886	**N16-H37**	σ*	1.95636	3.12	1.09	0.052
C9-C10	π	1.84522	**C7-C8**	π*	1.84120	11.24	0.31	0.053
C9-C13	σ	1.96741	**C7-C8**	π*	1.84120	3.33	1.26	0.058
C10-H33	σ	1.97807	**C8-C9**	σ*	1.96886	6.80	0.95	0.072
O11-C12	σ	1.98210	**C7-C8**	σ*	1.98007	3.85	1.42	0.066
C12-C13	σ	1.96624	**C9-C10**	σ*	1.97688	5.01	1.27	0.071
C12-H34	σ	1.96447	**C14-O15**	π*	1.98091	4.87	0.54	0.047
C14-N16	σ	1.98170	**N17-C18**	σ*	1.94446	2.84	1.35	0.055
N16-H37	σ	1.95636	**C24-H41**	π*	1.92377	10.00	1.14	0.095
N17-C18	π	1.94446	**C19-C20**	π*	1.78074	8.07	0.36	0.051
C19-C20	π	1.78074	**N17-C18**	π*	1.94446	13.92	0.29	0.057
C19-C24	σ	1.96628	**C23-O26**	σ*	1.98736	5.16	0.89	0.061
C20-C21	σ	1.97021	**C22-O25**	σ*	1.99212	5.50	0.88	0.062
C21-C22	π	1.79193	**C23-C24**	π*	1.97945	11.88	0.30	0.054
C21-H40	σ	1.97602	**C22-C23**	σ*	1.97582	6.20	0.90	0.067
C23-C24	π	1.82146	**C19-C20**	π*	1.78074	11.29	0.33	0.055
C24-H41	σ	1.92377	**N16-H37**	σ*	1.95636	26.57	0.99	0.145
O25-H42	σ	1.98582	**C21-C22**	σ*	1.79193	2.98	1.35	0.057
C27-H43	σ	1.98981	**C23-O26**	σ*	1.98736	3.66	0.82	0.049

3.7. Molecular Docking Studies

The method of molecular docking analysis is used to determine the affinities of chemical bonds to a receptor by enabling the determination of the proper binding geometries between a ligand and a target protein molecule [36]. Molecular docking analysis was performed with Maestro (version 11.8) [14]. The compound's protein crystal structure was chosen using the Protein Data Bank (http://www.rcsb.org). There are many protein targets on cancer. When we examine the literature, these two proteins have been widely used in cancer diseases [37, 38] We observed that we would obtain a good docking score when proteins were evaluated with reference ligands. Hydrogen atoms were added to the protein, and water molecules were eliminated throughout the preparation procedure using the protein preparation wizard. By clicking on any ligand atom, the Receptor Grid Creation application was launched, and the default grid box was created. Using Standard Precision, the ligand was attached to the protein grid box (SP). Docking scores were displayed as the results in Table 6. When we examined potential anticancer activity of HMFC compound against different proteins PDB ID: 1T46 and PDB ID: 3SXR, it is thought that the study with good docking scores is promising for these diseases and can make a significant contribution to new studies.

Table 6. Docking score of molecule HMFC PDB: 1T46 and PDB: 3SXR

Compound	Docking Score	
	(PDB: 1T46)	(PDB: 3SXR)
Molecule HMFC	-7.356	-6.866

Figure 6 shows 3D and 2D interactions as a result of Molecule-1T46 docking. The shift score with Molecule-1T46 was determined as -7.356 cal/mol in Table 6. In HMFC compound, THR-670 (4.12 Å) is the carbon-hydrogen bond linked to methoxy. CYS-673 (3.73 Å) on the Schiff base carbon is the conventional hydrogen bond. ASP-677 (4.54 Å) is a Pi-Anion bond on the naphthalene ring. In the benzene ring, VAL-603 (5.59 Å) is the Pi-Sigma bond. CYS-809 (4.12), ALA-621 (4.83), and LEU-799 (5.30) are Pi-Alkyl bonds in HMFC compound. GLY-676, GLU-671, and LYS-593 are van der Waals bonds in the binding mechanism of HMFC compound.

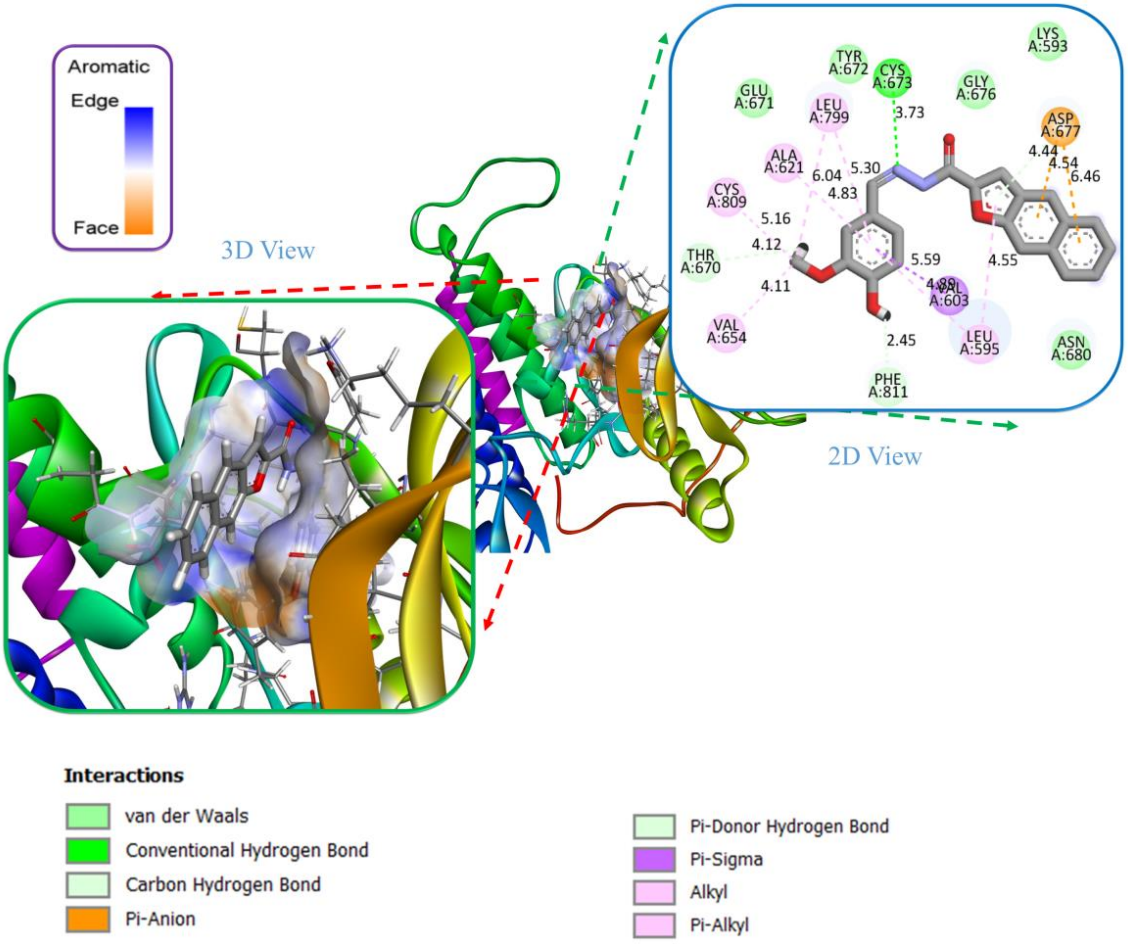

Figure 6. Molecule-1T46 mode of interaction with enzymes; a) 3D view of the donor/acceptor surface of aromatic bonds on the receptor b) 2D view of ligand enzyme interactions

Figure 7 shows 3D and 2D interactions as a result of Molecule-3SXR docking. The shift score with Molecule-3SXR was determined as -6.866 cal/mol in Table 6. VAL-431 (5.01 Å) is the Pi-Sigma bond on the naphthalene ring. In the benzene ring, CYS-496 (4.95 Å) is the Pi-Sulfur bond. In HMFC compound, LYS-445 (4.87), ALA-443 (6.48) and LEU-543 (5.97) are Pi-Alkyl bonds. GLY-429, SER-425 and MET-464 are van der Waals bonds in the binding mechanism of HMFC compound.

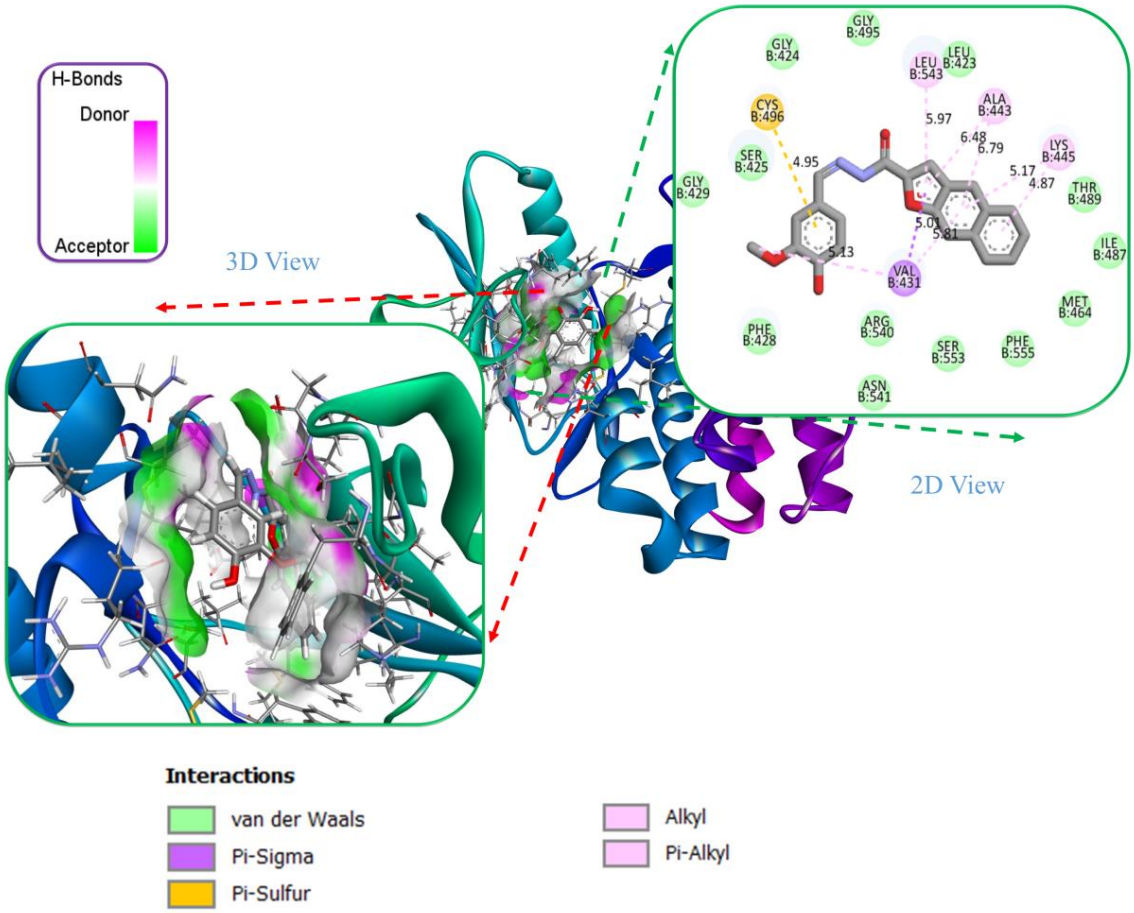

Figure 7. Ligand-3SXR mode of interaction with enzymes; 3D view of the donor/acceptor surface of hydrogen bonds on the receptor and 2D view of ligand enzyme interactions

3.8. ADME Analysis

Drug research and development heavily relies on the prediction of ADME characteristics. Early assessment of ADME characteristics reduces screening and trial time and costs by identifying the best candidates for drug development and rejecting those that are unlikely to succeed. By including kinetic mechanisms, the ultimate purpose of ADME modeling is to anticipate the in vivo propensity behavior of therapeutic candidate chemicals in the human body [39]. ADME analysis was performed to predict the ADME properties of HMFC molecule which is of great importance in drug research and development. Table 7 provides the following information about HMFC compound: molecular weight, percent absorption, topological polar surface region, estimated volume, number of rotatable bonds, and number of hydrogen bond donors and acceptors. When we examine the values in Table 7, according to Lipinski's five important rules; having less than 5 hydrogen bond donors (2), less than 10 hydrogen bond acceptors (5), lipophilicity coefficient LogP being less than 5 (3.46), molar refraction values between 4-130 (103.40) and finally We found that the molecular weight (MW) being lower than 500 (360.36) fits. It demonstrates that Lipinski's criteria has not been broken and that this molecule is appropriate for the drug development process. Using %A=109-(0.345xTPYA) to compute the percent absorption, the compounds had a decent absorption profile of 79.99%. The color regions and physicochemical parameters of molecule HMFC have been shown in Figure 8. When we examine Figure 8, The pink region on polar surface area maps symbolizes the physicochemical area suitable for oral bioavailability. According to the radar diagram, it is aside from the saturation setting, in the pink region. LogP is a measure of the lipophilicity or hydrophobicity of the compound. LogP > 0 indicates that the drug is

lipophilic and LogP < 0 indicates that the drug is hydrophilic. Since the compound has LogP >0 (3.46), it shows that the compound is lipophilic as a drug. According to Lipinski's rule, one of the most important chemical descriptors that correlates well with PK properties is the topological polar surface area (TPSA) and the TPSA of a good drug should be less than 140 Å. The TPSA value of HMFC compound was calculated as 84.06 and we think that it will be evaluated as a good drug candidate.

Table 7. Physicochemical and lipophilicity of molecule HMFC

Code DHPM	Lipophilicity consensus log P	Physico-chemical properties								
		MW[a] g/mol	Heavy Atoms	Aromatic heavy atoms	Rot. bond	H-acceptor bond	H-donor bond	MR[b]	TPSA[c] (A^2)	% ABS[d]
	3.46	360.36	27	19	5	5	2	103.40	84.06	79.99

[a]**MW**, molecular weight; [c]**TPSA**, topological polar surface area; [b]**MR**, molar refractivity; [d]**ABS%:** absorption percent $ABS\% = 109 - [0.345 \times TPSA]$.

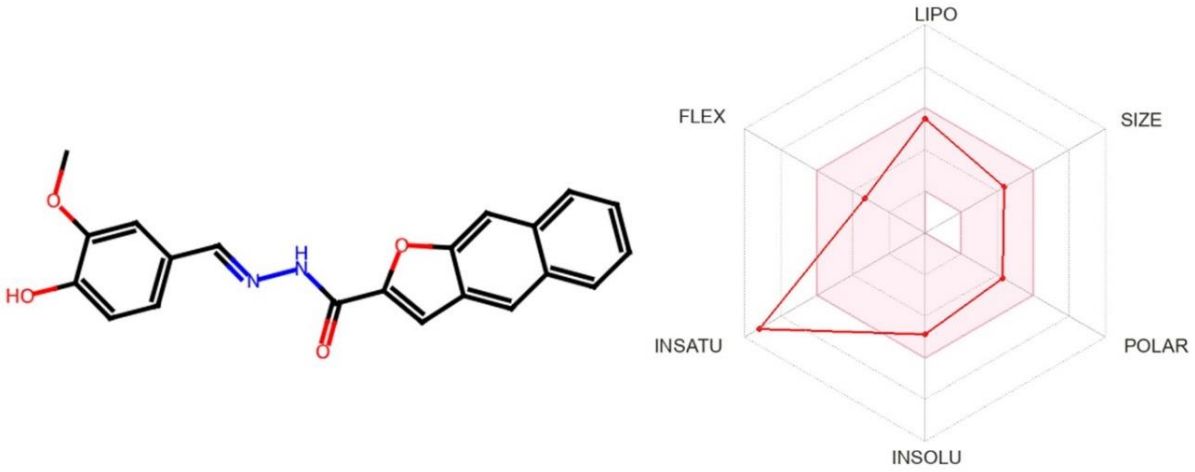

Figure 8. Color regions and physicochemical parameters of molecule HMFC

4. CONCLUSION

The initial step in HMFC investigation was to optimize the geometry to discover the least energy, or stable structure, of the molecule. The optimization process led to the determination of the molecule's bond lengths and bond angles. The molecule's total energies and leading molecular orbital energies were then calculated. These energies were used to calculate the molecular properties (η, or electronegativity, and η, or molecular stiffness), based on HOMO-LUMO energy differences. Examining the variations in NBO hybridization % and Mulliken and NBO atomic charge values, it was discovered that there were relatively few variations. The molecular electrostatic potential energy surface map (MEP) and nonlinear optical characteristics (polarizability, anisotropic polarizability, and high polarizability) were ascertained in order to provide further insight into the molecule under investigation. We were able to determine the regions where the compound might have non-covalent interactions by looking at the MEP map, which showed that the positive potential region was around the hydrogen and methyl atoms, and the negative potential region was around the electronegative atoms. HMFC compound's potential anticancer activity was tested on two different proteins, PDB ID: 1T46 and PDB ID: 3SXR. The optimum docking modes for the proteins PDB: 1T46 and PDB: 3SXR were found to have binding affinities of -7.356 kcal/mol and -6.866 kcal/mol, respectively, in the molecular docking study. Examining the two-dimensional view of the binding interactions to the residues in the molecular docking

analysis, it is evident that the interactions belong to the hydrogen bond, carbon-hydrogen bond, and van der Waals interactions and are active in the region with a high electrophilic nature. Finally, the HMFC investigation included molecular ADME analysis. According to the Adme research, it has an excellent absorption profile of 79.99%, and the field that produces safe and effective medications may find use for the study's findings.

CONFLICT OF INTEREST

There are no conflicts of interest as to publication of this article.

CRediT AUTHOR STATEMENT

Kenan Gören: Supervision, Writing-Review and Editing, **Mehmet Bağlan:** Research, Software, Writing-original draft, **Ümit Yıldıko:** Conceptualization, Formal analysis.

REFERENCES

[1] Raczuk E, Dmochowska B, Samaszko-Fiertek J and Madaj J. Different Schiff bases structure, importance and classification. Molecules. 2022; 27(3): 787.

[2] Ashraf MA, Mahmood K, Wajid A, Maah MJ and Yusoff I. Synthesis, characterization and biological activity of Schiff bases. IPCBEE. 2011; 10(1): 185.

[3] Da Silva CM, da Silva DL, Modolo LV, Alves RB, de Resende MA, Martins C V and de Fátima Â. Schiff bases: A short review of their antimicrobial activities. J. Adv. Res. 2011; 2(1): 1-8.

[4] El-Sonbati A, Mahmoud W, Mohamed GG, Diab M, Morgan SM and Abbas S. Synthesis, characterization of Schiff base metal complexes and their biological investigation. Appl. Organomet. Chem. 2019; 33(9): 5048.

[5] Dalia SA, Afsan F, Hossain MS, Khan MN, Zakaria C, Zahan M-E and Ali M. A short review on chemistry of schiff base metal complexes and their catalytic application. Int. J. Chem. Stud. 2018; 6(3): 2859-2867.

[6] Zhang J, Xu L and Wong W-Y. Energy materials based on metal Schiff base complexes. Coord. Chem. Rev. 2018; 355(180-198.

[7] Juyal VK, Pathak A, Panwar M, Thakuri SC, Prakash O, Agrwal A and Nand V. Schiff base metal complexes as a versatile catalyst: A review. J. Organomet. Chem. 2023; 122825.

[8] Hussain W, Amir A and Rasool N. Computer-aided study of selective flavonoids against chikungunya virus replication using molecular docking and DFT-based approach. Struct. Chem. 2020; 31: 1363-1374.

[9] Bubaš M, and Sancho-Parramon J. DFT-Based Approach Enables Deliberate Tuning of Alloy Nanostructure Plasmonic Properties. J. Phys. Chem. C. 2021; 125(43): 24032-24042.

[10] Gertig C, Leonhard K and Bardow A. Computer-aided molecular and processes design based on quantum chemistry: current status and future prospects. Curr. Opin. Chem. Eng. 2020; (27): 89-97.

[11] Liu Q, Tang K, Zhang J, Feng Y, Xu C, Liu L, Du J and Zhang L, QMaC: a quantum mechanics/machine learning-based computational tool for chemical product design, in Computer Aided Chemical Engineering. 2020, Elsevier. p. 1807-1812.

[12] Papadopoulos-A I, Tsivintzelis I, Linke P and Seferlis P. Computer aided molecular design: fundamentals, methods and applications. Chem., Mol. Sci. and Chem. Eng. 2018;

[13] T. Michael J. Frisch G W, Bernhard Schlegel, Gustavo Scuseria, 2016.

[14] Release S. 3: Maestro Schrödinger. LLC, New York 2019.

[15] Gören K, Bağlan M and Çakmak İ. Dietanol Amin Ditiyokarbamat RAFT Ajanının ^{1}H ve ^{13}C NMR Spektrumlarının Teorik İncelenmesi. J. Integr. Sci. Technol. 2022; 12(3): 1677-1689.

[16] Gören K, Bağlan M and Yıldıko Ü. Melanoma Cancer Evaluation with ADME and Molecular Docking Analysis, DFT Calculations of (E)-methyl 3-(1-(4-methoxybenzyl)-2,3-dioxoindolin-5-yl)-acrylate Molecule. JIST. 2024; 14(3): 1186-1199.

[16] Bağlan M, Gören K and Yıldıko Ü. HOMO–LUMO, NBO, NLO, MEP analysis and molecular docking using DFT calculations in DFPA molecule. Int. J. Chem. Technol. 2023; 7(1): 38-47.

[17] Kinaytürk NK. Elucidation of the Molecular Interaction Mechanism of Bromuconazole by DFT and Molecular Docking Methods. Süleyman Demirel Üniversitesi Fen Bilimleri Enstitüsü Dergisi. 2023; 27(2): 266-272.

[18] Saraç K. Synthesis and Theoretical Chemical Calculations of 4-Chloromethyl-6,8-dimethylcoumarin Compound. Bitlis Eren Üniversitesi Fen Bilimleri Dergisi. 2018; 7(2): 311-319.

[19] Gören K and Yıldıko Ü. Aldose Reductase Evaluation against Diabetic Complications Using ADME and Molecular Docking Studies and DFT Calculations of Spiroindoline Derivative Molecule. Süleyman Demirel Üniversitesi Fen Bilimleri Enstitüsü Dergisi. 2024; 28(2): 281-292.

[20] Bağlan M, Gören K and Yıldıko Ü. DFT Computations and Molecular Docking Studies of 3-(6-(3-aminophenyl) thiazolo [1, 2, 4] triazol-2-yl)-2H-chromen-2-one (ATTC) Molecule. HJSE. 2023; 10(1): 11-19.

[21] Gümüş HP, Tamer Ö, Avcı D and Atalay Y. 4-(Metoksimetil)-1,6-dimetil-2-okso-1,2-dihidropiridin-3-karbonitril molekülünün teorik olarak incelenmesi. Sakarya University Jounal of Science. 2015; 19(3): 303-311.

[22] Choudhary V, Bhatt A, Dash D and Sharma N. DFT calculations on molecular structures, HOMO–LUMO study, reactivity descriptors and spectral analyses of newly synthesized diorganotin (IV) 2-chloridophenylacetohydroxamate complexes. J. Comput. Chem. 2019; 40(27): 2354-2363.

[23] Mumit MA, Pal TK, Alam MA, Islam M, Paul S and Sheikh M C. DFT studies on vibrational and electronic spectra, HOMO–LUMO, MEP, HOMA, NBO and molecular docking analysis of benzyl-3-N-(2,4,5-trimethoxyphenylmethylene) hydrazinecarbodithioate. J. Mol. Struct. 2020; 1220(128715.

[24] Gören K, Bağlan M, Yıldıko Ü and Tahiroğlu V. Molecular Docking and DFT Analysis of Thiazolidinone-Bis Schiff Base for anti-Cancer and anti-Urease Activity. JIST. 2024; 14(2): 822-834.

[25] Bağlan M, Yıldıko Ü and Gören K. Computational Investigation of 5.5,7-trihydroxy-3,7-dimethoxy-4-4-O-biflavone from Flavonoids Using DFT Calculations and Molecular Docking. Adıyaman University Journal of Science. 2022; 12(2): 283-298.

[26] Lakshminarayanan S, Jeyasingh V, Murugesan K, Selvapalam N and Dass G. Molecular electrostatic potential (MEP) surface analysis of chemo sensors: An extra supporting hand for strength, selectivity & non-traditional interactions. J. Photochem. Photobiol. 2021; 6(100022.

[27] Bağlan M, Yıldıko Ü and Gören K. DFT Calculations and Molecular Docking Study in 6-(2"-Pyrrolıdınone-5"-Yl)-(-) Epicatechin Molecule From Flavonoids. Eskişehir Teknik Üniversitesi Bilim ve Teknoloji Dergisi B-Teorik Bilimler. 2023; 11(1): 43-55.

[28] Aziz A, Elantabli FM, Moustafa H, and El-Medani SM. Spectroscopic, DNA binding ability, biological activity, DFT calculations and non-linear optical properties (NLO) of novel Co (II), Cu (II), Zn (II), Cd (II) and Hg (II) complexes with ONS Schiff base. J. Mol. Struct. 2017; 1141(563-576.

[29] Gören K, Çimen E, Tahiroğlu V and Yıldıko Ü. Moleculer Docking and Theoretical Analysis of the (E)-5-((Z)-4-methylbenzylidene)-2-(((E)-4-methylbenzylidene)hydrazineylidene)-3-phenylthiazolidin-4-one Molecule. Bitlis Eren Üniversitesi Fen Bilimleri Dergisi. 2024; 13(3): 659-672.

[30] Shokr EK, Kamel MS, Abdel-Ghany H, Ali M and Abdou A. Synthesis, characterization, and DFT study of linear and non-linear optical properties of some novel thieno-[2, 3-b] thiophene azo dye derivatives. Mater. Chem. 2022; 290(126646.

[31] Khan AU, Khera RA, Anjum N, Shehzad RA, Iqbal S, Ayub K and Iqbal J. DFT study of superhalogen and superalkali doped graphitic carbon nitride and its non-linear optical properties. RSC advances. 2021; 11(14): 7779-7789.

[32] Tanriverdi A, Altun K, Yildiko Ü and Çakmak İ. Structural and spectral properties of 4-(4-(1-(4-Hydroxyphenyl)-1-phenylethyl)phenoxy)phthalonitrile: Analysis by TD-DFT method, ADME analysis and docking studies. Int. J. Chem. Technol. 2021; 5(2): 147-155.

[33] Demircioğlu Z, Kaştaş ÇA and Büyükgüngör O. The spectroscopic (FT-IR, UV–vis), Fukui function, NLO, NBO, NPA and tautomerism effect analysis of (E)-2-[(2-hydroxy-6-methoxybenzylidene) amino] benzonitrile. Mol. Biomol. Spectrosc. 2015; 139(539-548.

[34] Kazachenko AS, Akman F, Abdelmoulahi H, Issaoui N, Malyar YN, Al-Dossary O and Wojcik MJ. Intermolecular hydrogen bonds interactions in water clusters of ammonium sulfamate: FTIR, X-ray diffraction, AIM, DFT, RDG, ELF, NBO analysis. J. Mol. Liq. 2021; 342(117475.

[35] Pisano MB, Kumar A, Medda R, Gatto G, Pal R, Fais A, Era B, Cosentino S, Uriarte E and Santana L. Antibacterial activity and molecular docking studies of a selected series of hydroxy-3-arylcoumarins. Molecules. 2019; 24(15): 2815.

[36] Obuotor TM, Kolawole AO, Apalowo OE and Akamo AJ. Metabolic profiling, ADME pharmacokinetics, molecular docking studies and antibacterial potential of Phyllantus muellerianus leaves. Tradit. Med. 2023; 23(2): 427-442.

[37] Hamed IA, Ashida N and Nagamatsu T. Antitumor studies. Part 4: Design, synthesis, antitumor activity, and molecular docking study of novel 2-substituted 2-deoxoflavin-5-oxides, 2-deoxoalloxazine-5-oxides, and their 5-deaza analogs. BMCL. 2008; 16(2): 922-940.

[38] Liu F et al. Discovery of a Selective Irreversible BMX Inhibitor for Prostate Cancer. Chem. Biol. 2013; 8(7): 1423-1428.